Diamond-EuF_3 Nanocomposites with Bright Orange Photoluminescence

V. Sedov,[†,§,*], S. Kuznetsov[†],V. Ralchenko,[⊥,†,§], M. Mayakova[†], S. Savin,[‡] K. Zhuravlev,[‖] A. Martyanov,[†] I. Romanishkin, [†]A. Khomich, [‖]P. Fedorov[†], and V. Konov[†,§]

[†]*General Physics Institute RAS, Vavilov str. 38, Moscow 119991, Russia*

[§]*National Research Nuclear University MEPhI, Moscow 115409, Russia*

[⊥]*Harbin Institute of Technology, 92 Xidazhi Str., Harbin 150001, P.R. China*

[‡] *Moscow Technological University, Moscow 119454, Russia*
[‖]*Institute of Radio Engineering and Electronics RAS, Fryazino 141190, Russia*

ABSTRACT: We report the manufacturing of a novel diamond – rare earth (RE) composite material with EuF3 nanoparticles (NP) embedded in the synthesized microcrystalline diamond films that shows strong photoluminescence in the orange part of the visible spectrum. Synthesis of the aforementioned composite includes placement of EuF3 NP on the diamond substrate and subsequent coating of them with an additional polycrystalline diamond layer grown by microwave plasma chemical vapor deposition (CVD). The produced composite films exhibit high intensity localized photoluminescence (PL) at 612 nm generated by the EuF3 particles buried within very stable transparent diamond matrix. The proposed synthetic approach is quite versatile, as it allows preparation of the luminescent diamond - RE particles nanocomposites of different sizes and natures which perform well over a broad range of the visible spectrum.

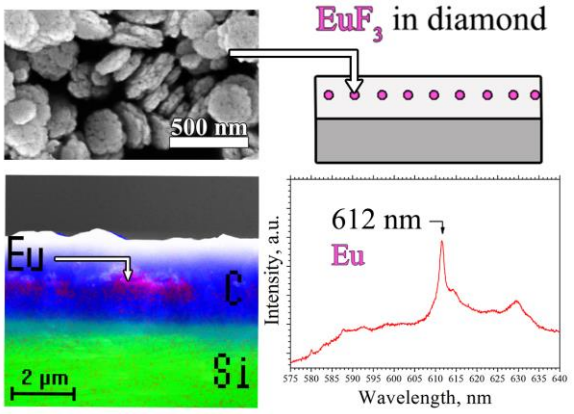

KEYWORDS: *diamond film, photoluminescence, rare earths, europium fluoride, nanoparticles*

Diamond nanophotonics is an area of modern materials science of increasing interest. This field has applications in quantum information technologies,[1-5] optical biomarkers,[6] and scintillators (X-ray beam monitors).[7,8] Extensive efforts in this field are focused at the impurity-related color centers in diamond (e.g., nitrogen-vacancy (NV),[9] silicon-vacancy (SiV),[10] germanium-vacancy (GeV),[11,12] chromium- or nickel-related defects,[13] etc.), that typically show

narrow (a few nanometers at room temperature) zero phonon lines (ZPL) in photoluminescence (PL) spectra and short PL decay times on the order of nanoseconds. These color centers can be easily produced by ion implantation in diamond[14] or by chemical vapor deposition (CVD) with *in situ* doping.[10,15] While known PL properties of the impurity-vacancy centers are quite suitable for engineering single photon emitters, the search for new and better PL sources in a diamond matrix, which could extend their spectral range and increase their decay time and efficiency, is still an ongoing activity. In particular, their PL emission could be further improved using rare earth (RE) ions, which are known for their higher quantum efficiency and longer PL decay times in the millisecond range.[16] The latter assumption is based on the well-established use of the RE-doped phosphors in white light-emitting devices,[17,18] plasma display panels, field emission displays, solar cells,[16] X-ray scintillators,[19,20] etc. Composite luminescent materials with rare-earth fluoride nanoparticles incorporated into oxide glass matrices are also widely implemented.[21] The ideas presented above suggest that the promising combination of chemical stability and lack of diamond cytotoxicity with the unique optical properties of rare earth ions could be crucially important for the development of RE-doped diamond materials which can be successfully utilized as brighter bio-markers[22,23] and X-ray imagers.[7,24] However, the direct incorporation of the large RE ions in the diamond crystal lattice (the densest among solid materials) is very difficult from technical point of view; recently, Magyar et al.[25] reported the first such attempt to introduce RE atoms into a diamond lattice by doping diamond single crystals with europium (Eu^{3+}) nanoparticles (NP). The authors attached via multistep chemical process Eu(III) tri-(2,6-pyridine dicarboxylic acid) complex (EuDPA) to the polymer layer, assembled on the diamond substrate, and then proceeded with diamond deposition to cover the Eu-containing molecules with an outer diamond layer. The obtained material exhibited Eu fluorescence with typical intensive line(s) at 612 nm, but Eu/diamond fluorescence was different than that of the precursor EuDPA complex, with the strongest precursor singlet peak $^5D_0 \rightarrow {}^7F_2$ becoming a multiplet, and broadening and/or splitting of $^5D_0 \rightarrow {}^7F_1$ and $^5D_0 \rightarrow {}^7F_4$ transitions also appearing in the PL spectra. While Magyar et al.[25] simulated the energy levels of the Eu defect within the diamond lattice and found, that substitutional atom state can be stable, no direct confirmation about the state of Eu in diamond was given. Since Eu(III) readily forms oxides, one may not exclude the formation of Eu-containing NP in their experiment, but the question whether RE can be immersed in the diamond lattice as a single ion still remains to be answered.

Our paper describes an alternative approach to incorporate RE elements in diamond by imbedding europium fluoride EuF_3 NP in chemical vapor deposition-grown diamond film and, thus, prepare a composite with the mechanically strong and chemically transparent inert matrix,

having the properties inherent to diamond, while retaining the excellent PL properties of EuF_3 particles. Our method allows the manufacture of such diamond-based composites not only just with the one rare earth element, but also with the mixture of several RE metals, in order to fine-tune the PL emission spectrum range.

Europium trifluoride (EuF_3) has been chosen as the primary object for our studies because of its non-toxic and moisture-resistant nature in comparison with other RE chalcogenides, iodides, bromides and chlorides. Also, EuF_3 possesses higher isomorphic capacity and lower phonon energy than RE oxides. EuF_3 exists in two polymorphs: a higher temperature hexagonal tysonite-type α-modification, and a lower temperature orthorhombic β-YF_3 modification.[26] We prepared hexagonal tysonite-type EuF_3 nanopowder via precipitation from aqueous europium nitrate solutions with aqueous hydrofluoric acid under ambient conditions[27,28] (see Methods in Supporting Information). A typical X-ray diffraction (XRD) pattern of the synthesized single-phase EuF_3 nanopowder with hexagonal tysonite structure (P-3c1 space symmetry group; a = 6.9191(1), c = 7.0967(1) Å lattice parameters; coherent scattering domain size is about 37 nm; Fig. 1) is in complete agreement with literature data (JCPDS card 32-0373); no other crystalline phase has been detected. It is worth mentioning that the preparation of the non-equilibrium higher temperature phase at room temperature is a quite common phenomenon in nanotechnology.[29] The study of the EuF_3 particle size distribution in an aqueous suspension by dynamic light scattering revealed that it contained mainly single particles with mean size (diameter) of about 220 nm and minor fraction of agglomerates with mean size of about 500 nm (for further study details, please see Methods section in the Supporting Information).

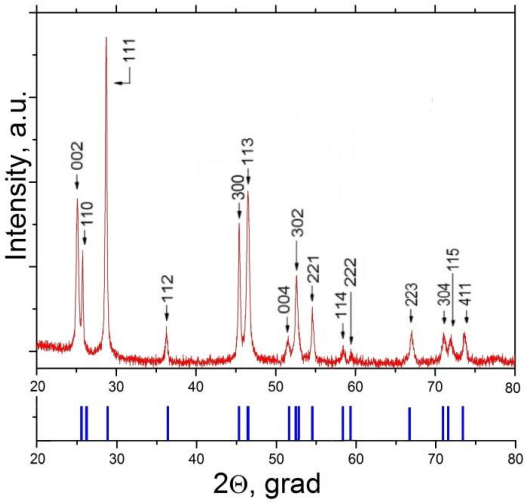

Figure 1. X-ray diffraction pattern of tysonite-type EuF_3 nano-powder (CuK_α radiation; literature data for the reflection angles are presented as blue bars below for comparison).

The synthetic scheme for diamond-EuF_3 composite preparation is shown in Fig. 2. At the beginning, the 20 × 20 × 0.5 mm^3 polished (100) single crystal Si wafers, used as the substrates, were seeded with detonation nanodiamonds (average size about 5 nm) in a water-based slurry. Then, ca. 1.2 μm thick primary microcrystalline diamond film was generated by microwave plasma chemical vapor deposition (CVD) in CH_4(5%)/H_2 gas mixture (800^{o}C substrate temperature; for further details, see Methods in Supporting Information) and the formed diamond film was seeded with the EuF_3 NP from an aqueous slurry (0.1 wt% EuF_3) using a spin-coating technique (1 EuF_3 particle per 10 μm^2). In the next step, additional diamond deposition was continued in order to add the second ca. 1.2 μm thick microcrystalline diamond layer on the top of the primary film, thus encapsulating the EuF_3 particles.

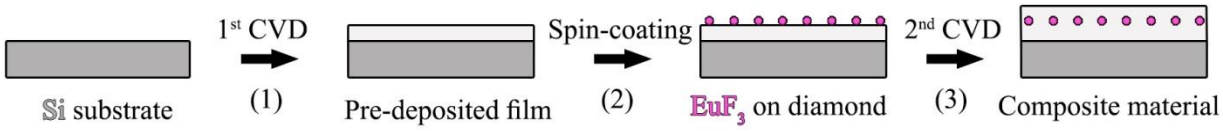

Figure 2. The scheme of diamond composite preparation by imbedding EuF_3 nanoparticles between two microcrystalline diamond films on the silicon substrate.

Scanning electron microscope (SEM) study of the synthesized EuF_3 (Fig. 3a) revealed disk-shaped agglomerates (ca. 100 nm thick, and 300 nm in diameter) consisting of ca. 40 nm primary NPs. The latter value of primary NP size is in excellent agreement with the size of coherent scattering domains (ca. 37 nm) assessed from the XRD data with the use of the Scherrer equation. One such primary EuF_3 particle, seeded on a pre-deposited diamond film with grain size ca. 400 nm, is shown in Fig.3b. After repeated diamond deposition for 40 minutes, EuF_3 NPs were completely overgrown, and the diamond grain size has been enlarged up to about 1 μm (Fig. 3c). It is worth noting that the used RE fluoride preparation method for synthesizing starting 37 nm europium nanofluoride allows reduction of the initial RE particle size down to several tens of nanometers if necessary (as has been reported, for example, for LaF_3:Yb:Er[28-30]).

The position of EuF_3 particles inside the diamond film(s) can be easily identified in the SEM image of the sample's fractured surface (Fig. 3d): the first diamond layer had a columnar structure with continuously increasing grain size, having a fine-grained layer with encapsulated EuF_3 NPs, followed by the 2-nd diamond layer on the top. Energy-dispersive X-ray spectroscopy (EDX) of the same cross-section clearly showed a strong Eu signal in the central region of the film (Fig. 3e), additionally confirming the incorporation of EuF_3 NP in diamond bulk.

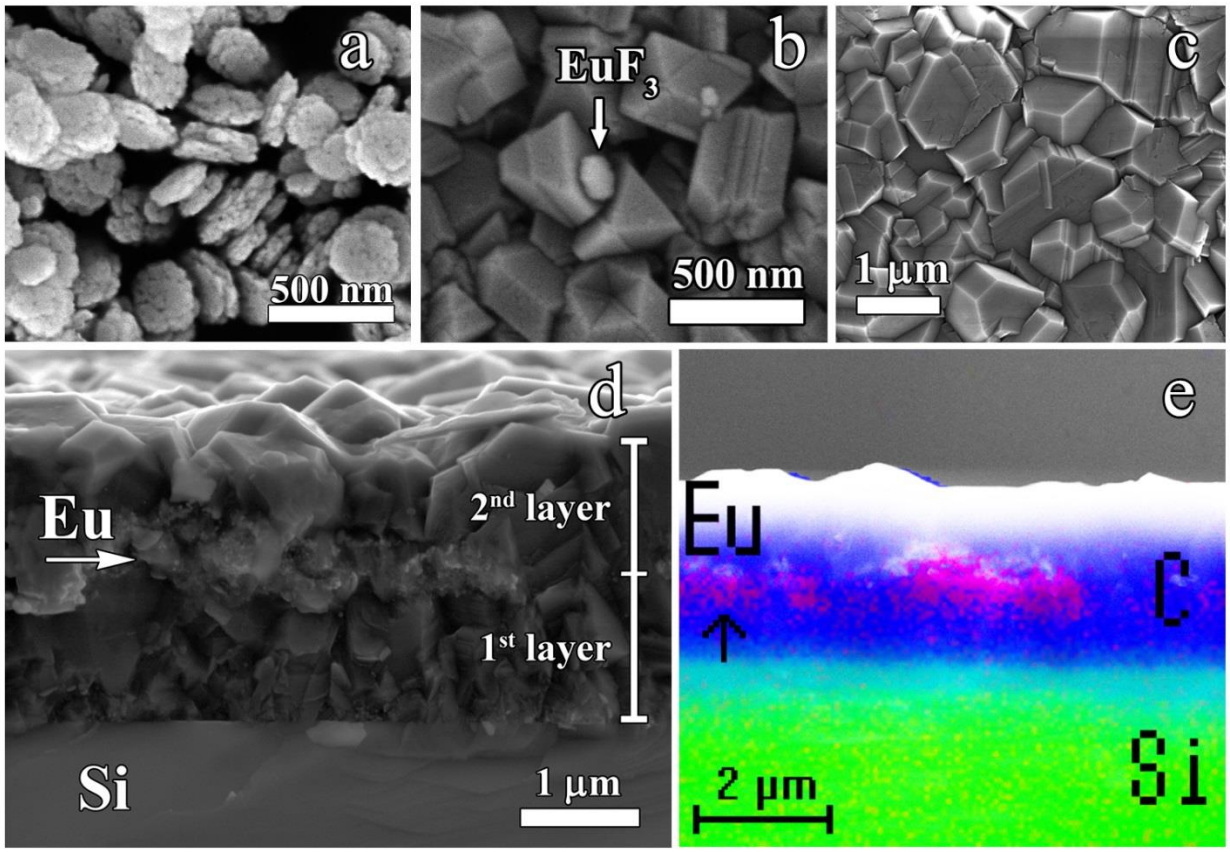

Figure 3. SEM images (top views) of synthesized EuF_3 nano-powder (a), the seeded EuF_3 particles on a pre-deposited diamond film (b), and the surface of 2nd diamond film after 40 min CVD growth on the top of EuF_3 particles (c). SEM image of cross-section of the diamond film with imbedded EuF_3 particles in the middle of the film (d). EDX mapping of elements across the same cross-section (e): green layer – silicon, blue layer – carbon, purple dots – europium (also shown by arrow).

The typical PL spectrum (550-725 nm) for the freshly-prepared EuF_3 nanopowder (Fig. 4a) contains five lines associated with $^5D_0$-^7F_n transitions (n = 0-4) with the $^5D_0 \rightarrow {}^7F_1$ magnetic-dipole transition dominating. The intensity of the forced electrical dipole transition $^5D_0 \rightarrow {}^7F_2$, which is very sensitive to the local environment, is notably lower, and the latter suggests a high symmetry of the crystal field for Eu^{3+} ions.[31]

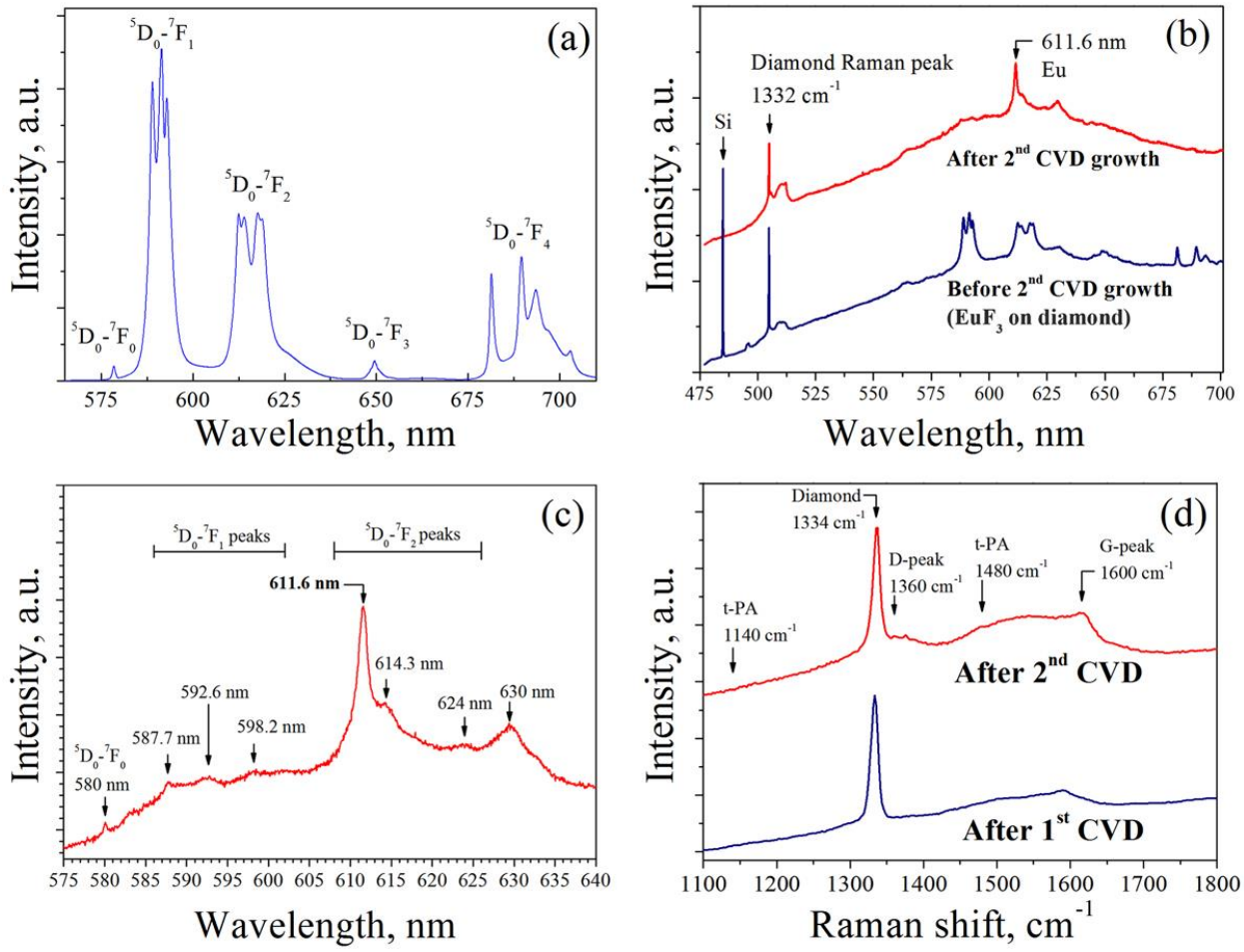

Figure 4. PL spectrum of synthesized EuF_3 powder (λ_{exc} = 473 nm) (a). PL spectra for pre-deposited diamond film seeded with EuF_3 particles (bottom spectrum) and for diamond film after 40 min CVD growth with embedded EuF_3 NP (top spectrum) (b). Broadening of the PL line between 575 nm and 675 nm was caused by NV^0 nitrogen-vacancy, NV^- defects and amorphous carbon impurity. The narrow lines at 486 nm and 505 nm are Raman peaks for silicon substrate and diamond, respectively. The strong 611.6 nm peak corresponds to the Eu^{+3} $^5D_0 \rightarrow {}^7F_2$ transition, while the appearance of the 630 nm line is caused by a specific CVD diamond defect. The high resolution PL spectrum for the EuF_3 component in the composite film is shown in (c), while the Raman spectra for the pre-deposited diamond film (bottom) and the film containing EuF_3 NP after the 2nd 40 min growth (top) are in (d). All spectra were recorded at the 473 nm excitation wavelength at room temperature.

The PL spectrum for the embedded EuF_3 NPs is distinctly different from the corresponding starting EuF_3 on the diamond nano-powder spectrum (Fig. 4b). The only common Eu-related feature in these spectra is the narrow line at 611.6 nm which corresponds to the $^5D_0 \rightarrow 7F_2$ transition. The pre-deposited diamond film showed no peak at this wavelength (Fig. 4b;

bottom spectrum). Another line at 630 nm belongs to a defect of unknown nature related to the CVD diamond[32] and unrelated to EuF_3, for it is also present in the pre-deposited diamond film. The 611.6 nm PL line in the composite is very narrow, with its full width at its half magnitude (FWHM) at only approximately 1.6 nm (Fig. 4c), i. e., far less than for the other Eu-based materials.[33,34] The two weak peaks at longer wavelengths, λ= 614.3 nm and 624.0 nm, also correspond to the $^5D_0$ - $^7F_2$ transition, but they are far less intense. Also, strongly damped, yet visible, are the lines for the $^5D_0$ - $^7F_1$ transition. Thus, the domination of $^5D_0$-$^7F_2$ transition in the imbedded EuF_3 particles suggests that the symmetry of the local environment around the Eu was lower than its symmetry in the isolated NPs. A similar effect has been observed by Magyar et al.[25] for the cathodoluminescence of Eu defects in nanodiamonds: an intense and broad 612 nm line (FWHM ca. 20 nm) along with strongly-damped lines corresponding to the other transitions.

In our experiments, apparently, changes in the Eu ion environment have occurred at the boundaries of EuF_3 NPs due to their interaction with carbon atoms. However, since only a minority of all Eu atoms were located at these boundaries, the latter factor alone is unlikely to be responsible for the observed PL spectrum modification. Diamond deposition occurred in an essentially hydrogen-rich plasma in the presence of active atomic hydrogen, so EuF_3 reaction with hydrogen at higher temperature might have resulted in the formation of intermediate-ordered phases such as hexagonal $EuF_{2.40}$ (JCPDS card 26-0626) or tetragonal $EuF_{2.25}$ (JCPDS card 26-0625), or via a polymorphic transformation to low symmetry orthorhombic EuF_3 (JCPDS card 33-0542), thus, lowering the higher original site symmetry of Eu atoms (such transformations of rare earth fluorides are well known[35-37]). Another reason for the appearance of asymmetry in the inner coordination sphere of Eu atoms may be a biaxial thermal compressive stress in the diamond film (according to our estimate, ca. 0.25 GPa) due to a mismatch between the thermal expansion coefficients (TEC) for diamond (0.8×10^{-6} K^{-1} at room temperature) and the silicon substrate, resulting in a stress in the encapsulated EuF_3 particles. Also, the thermal stress in EuF_3 particles might originate from a mismatch in the TECs for diamond and fluoride. The TEC for the europium fluoride is not known to us, but it can be roughly estimated to be equal to that of lanthanum fluoride (8.7×10^{-6} K^{-1} at 100-300 ^oC).

The features of the Raman spectra for the diamond films (Fig. 4d) include a narrow (FWHM ca. 10 cm^{-1}) diamond peak at about 1334 cm^{-1}, broad D- and G-lines from sp^2-bonded amorphous carbon (a-C) at 1350 cm^{-1} and 1580 cm^{-1}, respectively, and the lines at 1140 cm^{-1} and 1450 cm^{-1} corresponding to *trans*-polyacetylene (t-PA).[38,39] The a-C and t-PA components are located at hydrogen-tethered grain boundaries, including EuF_3-diamond interfaces. We estimate that the fluoride-diamond interface could be more regular/ordered for EuF_3 NPs embedded in

single crystal diamond compared to the polycrystalline specimens described in the present paper (the experiments on preparation of such composites are in progress now).

In conclusion, we have prepared and characterized diamond-rare earth composite materials with EuF_3 NP embedded in microcrystalline CVD diamond films that exhibit photoluminescence emission at about 612 nm. We have developed a novel and very flexible technique that can be easily implemented for other rare earth and alkaline earth fluorides and/or oxides, so the latter species with unique optical and magnetic properties, including effective up-conversion and X-ray luminescence nanoparticles, can be easily incorporated into a polycrystalline diamond matrix. Our method can also be applied for the preparation of the multilayered composites with the same or different RE nanoparticles accommodated in their own layer(s) via repeated multiple-time diamond deposition. Alternatively, it is possible to seed a mixture of different RE species on the substrate surface to enhance the intensity and/or broaden spectral range of the PL emission to produce a multicolor light source. The luminescent properties of such composites can be further improved in order to reduce the background PL from non-diamond carbon by using a single crystal diamond substrate (instead of the polycrystalline one) to embed the RE NPs within the epitaxially grown diamond film. In addition, our method allows the use of such smaller lantanide fluoride particles (as small as a few tens nanometers[40]), so this would enhance their localization within the diamond matrix.

ASSOCIATED CONTENT

Supporting Information

Synthesis (preparation of EuF_3 particles, diamond film deposition) and characterization (X-ray diffraction, scanning electron microscopy, Raman and photoluminescence analysis, dynamic light scattering, nano-particle size distribution (Figure S1)).

AUTHOR INFORMATION

Corresponding Author: Vadim Sedov

*Phone: +7-499-503-87-81. Fax: +7 (499) 135-0270. E-mail: sedovvadim@yandex.ru.

Notes

Authors declare no competing financial interest.

ACKNOWLEDGMENTS

This work was supported by the Russian Science Foundation, grant No. 14-22-00243.

REFERENCES

(1) Prawer, S.; Aharonovich, I. *Quantum Information Processing with Diamond: Principles and Applications*; Elsevier, 2014.

(2) Aharonovich, I.; Neu, E. *Advanced Optical Materials* **2014**, *2* (10), 911–928.

(3) Aharonovich, I.; Greentree, A. D.; Prawer, S. *Nat Photon* **2011**, *5* (7), 397–405.

(4) Riedrich-Möller, J.; Arend, C.; Pauly, C.; Mücklich, F.; Fischer, M.; Gsell, S.; Schreck, M.; Becher, C. *Nano Lett.* **2014**, *14* (9), 5281–5287.

(5) Li, L.; Chen, E. H.; Zheng, J.; Mouradian, S. L.; Dolde, F.; Schröder, T.; Karaveli, S.; Markham, M. L.; Twitchen, D. J.; Englund, D. *Nano Lett.* **2015**, *15* (3), 1493–1497.

(6) Merson, T. D.; Castelletto, S.; Aharonovich, I.; Turbic, A.; Kilpatrick, T. J.; Turnley, A. M. *Optics Letters* **2013**, *38* (20), 4170.

(7) Kudo, T.; Takahashi, S.; Nariyama, N.; Hirono, T.; Tachibana, T.; Kitamura, H. *Review of Scientific Instruments* **2006**, *77* (12), 123105.

(8) Degenhardt, M.; Aprigliano, G.; Schulte-Schrepping, H.; Hahn, U.; Grabosch, H.-J.; Wörner, E. *J. Phys.: Conf. Ser.* **2013**, *425* (19), 192022.

(9) Schirhagl, R.; Chang, K.; Loretz, M.; Degen, C. L. *Annual Review of Physical Chemistry* **2014**, *65* (1), 83–105.

(10) Neu, E.; Steinmetz, D.; Riedrich-Möller, J.; Gsell, S.; Fischer, M.; Matthias Schreck; Becher, C. *New J. Phys.* **2011**, *13* (2), 025012.

(11) Ralchenko, V. G.; Sedov, V. S.; Khomich, A. A.; Krivobok, V. S.; Nikolaev, S. N.; Savin, S. S.; Vlasov, I. I.; Konov, V. I. *Bulletin of the Lebedev Physics Institute* **2015**, *42* (6), 165–168.

(12) Ekimov, E. A.; Lyapin, S. G.; Boldyrev, K. N.; Kondrin, M. V.; Khmelnitskiy, R.; Gavva, V. A.; Kotereva, T. V.; Popova, M. N. *Письма в ЖЭТФ* **2015**, *102* (11-12), 811.

(13) Aharonovich, I.; Castelletto, S.; Johnson, B. C.; McCallum, J. C.; Simpson, D. A.; Greentree, A. D.; Prawer, S. *Phys. Rev. B* **2010**, *81* (12), 121201.

(14) Pezzagna, S.; Rogalla, D.; Wildanger, D.; Meijer, J.; Zaitsev, A. *New J. Phys.* **2011**, *13* (3), 035024.

(15) Bolshakov, A.; Ralchenko, V.; Sedov, V.; Khomich, A.; Vlasov, I.; Khomich, A.; Trofimov, N.; Krivobok, V.; Nikolaev, S.; Khmelnitskii, R.; others. *physica status solidi (a)* **2015**, *212* (11), 2525–2532.

(16) Huang, X.; Han, S.; Huang, W.; Liu, X. *Chemical Society Reviews* **2013**, *42* (1), 173–201.

(17) Rozhnova, Y. A.; Luginina, A. A.; Voronov, V. V.; Ermakov, R. P.; Kuznetsov, S. V.; Ryabova, A. V.; Pominova, D. V.; Arbenina, V. V.; Osiko, V. V.; Fedorov, P. P. *Materials Chemistry and Physics* **2014**, *148* (1), 201–207.

(18) Hölsä, J.; Laamanen, T.; Laihinen, T.; Lastusaari, M.; Pihlgren, L.; Rodrigues, L. C. *Optical Materials* **2014**, *36* (10), 1627–1630.

(19) Lin, C. C.; Liu, R.-S. *The journal of physical chemistry letters* **2011**, *2* (11), 1268–1277.

(20) Yanagida, T. *Optical Materials* **2013**, *35* (11), 1987–1992.

(21) P.P. Fedorov, A.A. Luginina, A.I. Popov. Transparent Oxyfluoride Glass Ceramics. // J. Fluorine Chem. Vol. 172, pp. 22-50 (2015).

(22) Hui, Y. Y.; Cheng, C.-L.; Chang, H.-C. *Journal of Physics D: Applied Physics* **2010**, *43* (37), 374021.

(23) Wang, F.; Banerjee, D.; Liu, Y.; Chen, X.; Liu, X. *Analyst* **2010**, *135* (8), 1839–1854.

(24) Tono, K.; Togashi, T.; Inubushi, Y.; Sato, T.; Katayama, T.; Ogawa, K.; Ohashi, H.; Kimura, H.; Takahashi, S.; Takeshita, K.; others. *New Journal of Physics* **2013**, *15* (8), 083035.

(25) Magyar, A.; Hu, W.; Shanley, T.; Flatté, M. E.; Hu, E.; Aharonovich, I. *Nature communications* **2014**, *5*. article 3523.

(26) Sobolev, B. P. *The Rare Earth Trifluorides: The high temperature chemistry of the rare earth trifluorides*; Institutd'Estudis Catalans, 2000; Part 1.
(27) P.P. Fedorov, A.A. Luginina, S.V. Kuznetsov, V.V. Osiko. *J. Fluorine Chem.* **2011**. 132. 1012-1039.
(28) Fedorov, P. P.; Osiko, V. V.; Kuznetsov, S. V.; Uvarov, O. V.; Mayakova, M. N.; Yasirkina, D. S.; Ovsyannikova, A. A.; Voronov, V. V.; Ivanov, V. K. *Journal of Crystal Growth* **2014**, *401*, 63–66.
(29) Fedorov P.P., Kuznetsov S.V., Osiko V.V. Elaboration of nanofluorides and ceramics for optical and laser applications / Chapter in the book "Photonic & Electronic Properties of Fluoride Materials" Ed. A. Tressaud, K. Popelmeier, 2016 Elsevier
(30) Fedorov P.P.; Mayakova M.N.; Kuznetsov S.V. et all *Materials Research Bulletin*. **2012**. 47. 1794-1799.
(31) Volanti, D. P.; Rosa, I. L.; Paris, E. C.; Paskocimas, C. A.; Pizani, P. S.; Varela, J. A.; Longo, E. Optical Materials **2009**, 31 (6), 995–999.
(32) Zaitsev, A. M. Optical properties of diamond: a data handbook; Springer Science & Business Media, 2013.
(33) O'Riordan, A.; O'Connor, E.; Moynihan, S.; Llinares, X.; Van Deun, R.; Fias, P.; Nockemann, P.; Binnemans, K.; Redmond, G. Thin Solid Films **2005**, 491 (1), 264–269.
(34) Sun, W.; Yu, J.; Deng, R.; Rong, Y.; Fujimoto, B.; Wu, C.; Zhang, H.; Chiu, D. T. Angewandte Chemie (International ed. in English) **2013**, 52 (43).
(35) O. Greis J. Solid State Chemistry. **1978**. 24. 227-232
(36) T. Petzel, O. Greis Z. anorg. Allg. Chem. **1972** 388 137-157
(37) Kaczmarek, S. M.; Tsuboi, T.; Ito, M.; Boulon, G.; Leniec, G. J. Phys.: Condens. Matter **2005**, 17 (25), 3771.
(38) Vlasov, I. I.; Goovaerts, E.; Ralchenko, V. G.; Konov, V. I.; Khomich, A. V.; Kanzyuba, M. V. Diamond and Related Materials **2007**, 16 (12), 2074–2077.
(39) Sedov, V.; Ralchenko, V.; Khomich, A. A.; Vlasov, I.; Vul, A.; Savin, S.; Goryachev, A.; Konov, V. Diamond and Related Materials **2015**, 56, 23–28.
(40) Chan, E. M.; Han, G.; Goldberg, J. D.; Gargas, D. J.; Ostrowski, A. D.; Schuck, P. J.; Cohen, B. E.; Milliron, D. J. Nano Lett. **2012**, 12 (7), 3839–3845.